Phosphorus Cations

DOI: 10.1002/ange.200501850

Small Cyclopolyphosphinophosphonium Cations: Systematic Development of Fundamental *catena*-Phosphorus Frameworks**

Neil Burford, C. Adam Dyker, Mike Lumsden, and Andreas Decken*

Recognizing that catenation of carbon is principally responsible for the diversity and extent of organic chemistry, the "diagonal relationship" between carbon and phosphorus in the Periodic Table is often quoted[1,2] in the discussion of the numerous catenated polyphosphines[2–6] and polyphosphorus anions.[2–4,7–12] *catena*-Phosphorus cation systems are less well developed despite the classical chemistry of phosphonium salts, but the pioneering contributions of Schmidpeter and coworkers[13–15] and Schmutzler et al.[16] have highlighted new aspects of structure and bonding that prompt the establishment of a comprehensive polyphosphinophosphonium series. Our high-yielding and facile methods for the synthesis of the prototypical phosphinophosphonium **1**,[17] diphosphinophosphonium **2**,[18] and cyclotetraphosphinophosphonium **5**[18] cations have now been applied to the preparation of the first examples of cyclodiphosphinophosphonium **3** and cyclotriphosphinophosphonium **4** cations (Scheme 1). Isolation of these new frameworks is surprising in light of the exclusive formation of **5** over possible tetra- and hexaphosphorus derivatives with phenyl substituents at the phosphorus centers.[18] Derivatives of **3** and **4** provide representative frameworks that complete a series of the smallest cyclopolyphosphinophosphonium cations **3**–**5**, and their characterization is pivotal in the systematic development of fundamental phosphorus chemistry.

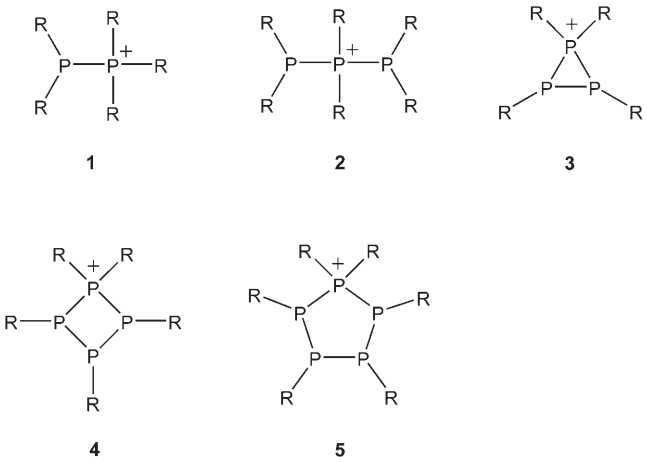

Scheme 1. Prototypical *catena*-polyphosphinophosphonium cation frameworks.

^{31}P NMR spectra of reaction mixtures containing (P*t*Bu)$_3$ (**6a**) with excess MeOTf show quantitative formation of [(P*t*Bu)$_3$Me][OTf] (**3a**-OTf; Figure 1a and Scheme 2a). The spectrum can be approximated as an AMX[19] spin system and is consistent with the solid-state structure of **3a**-OTf (Figure 2a), thus demonstrating stereoselective methylation of **6a** at either of the *syn*-configured centers to give a racemic

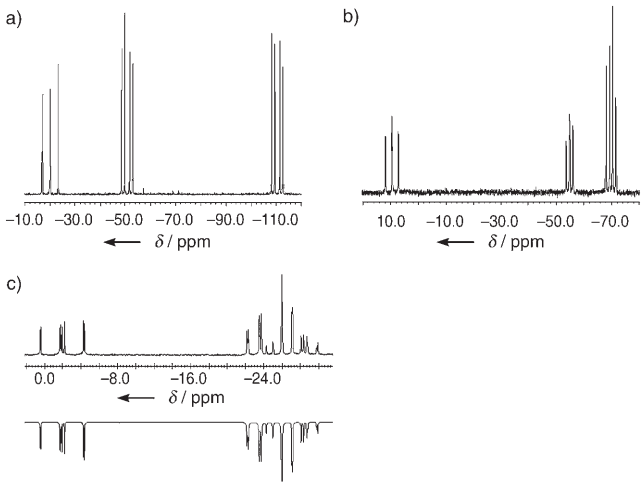

Figure 1. ^{31}P NMR spectra at 101.3 MHz: a) mixture of MeOTf (2 equiv) and (P*t*Bu)$_3$, which shows the approximate AMX pattern of **3a**-OTf; b) mixture of MeOTf (2 equiv) and (PCy)$_4$, which shows the approximate A$_2$MX pattern of **4a**-OTf; c) experimental (top) and simulated (inverted) AB$_2$X pattern of pure **4b**-OTf.

[*] Prof. N. Burford, C. A. Dyker
Department of Chemistry
Dalhousie University
Halifax, NS, B3H 4J3 (Canada)
Fax: (+1) 905-494-1310
E-mail: neil.burford@dal.ca
Dr. M. Lumsden
Atlantic Region Magnetic Resonance Center
Dalhousie University
Halifax, NS, B3H 4J3 (Canada)
Dr. A. Decken
Department of Chemistry
University of New Brunswick
Fredericton, NB, E3A 6E2 (Canada)

[**] We thank the Natural Sciences and Engineering Research Council of Canada, the Killam Foundation, the Canada Research Chairs Program, the Canada Foundation for Innovation, the Nova Scotia Research and Innovation Trust Fund, and the Walter C. Sumner Foundation for funding.

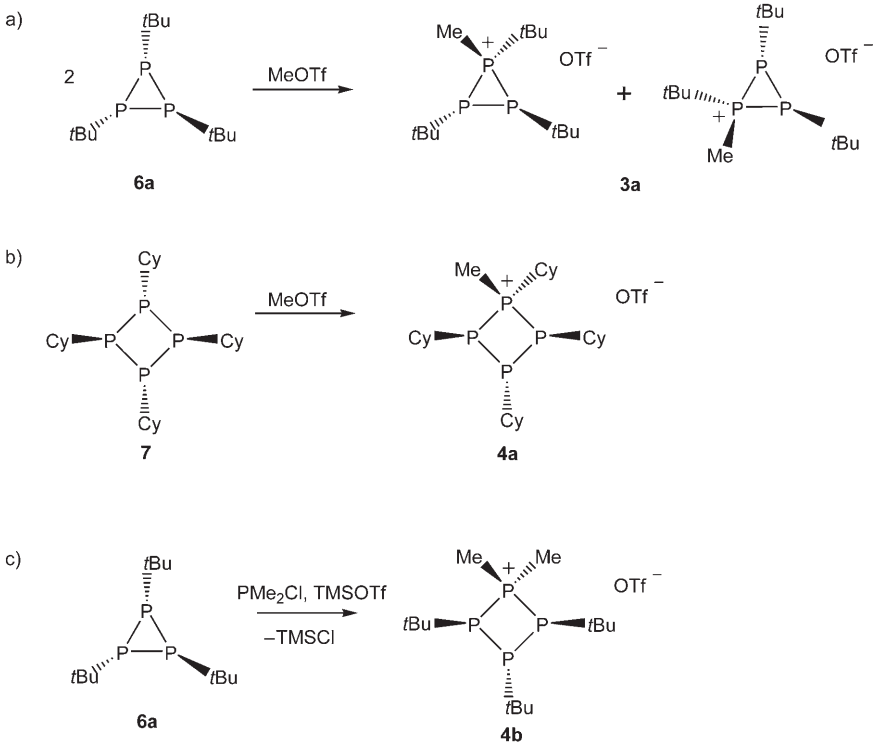

Scheme 2. Preparation of cyclopolyphosphinophosphonium cations. OTf = trifluoromethanesulfonate, Cy = cyclohexyl, TMS = trimethylsilyl.

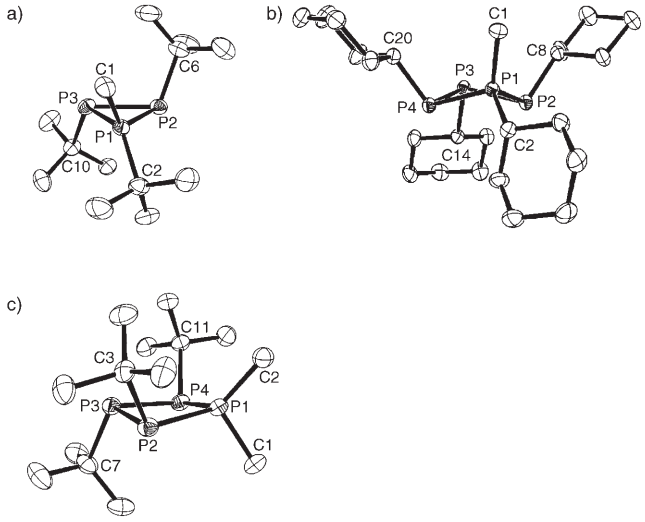

Figure 2. Representative structural views of the cations in a) **3a**-OTf, b) **4a**-OTf, and c) **4b**-OTf. Ellipsoids are given at the 50% probability level. Hydrogen atoms are omitted for clarity.

mixture rather than the *meso* isomer. Similarly, the homocyclic tetraphosphorus core is maintained in the formation of [(PCy)$_4$Me][OTf] (**4a**-OTf) from (PCy)$_4$ (**7**) and MeOTf (Scheme 2b), and the ^{31}P NMR spectrum of the reaction mixture can be approximated as an A_2MX spin system (Figure 1b). Thus, methylation occurs at one of the four equivalent phosphorus atoms in the all-*trans* configuration of **7**, which is confirmed by the solid-state structure of the *meso* isomer **4a** (Figure 2b). The reaction of **6a** with 1.5 equivalents of PMe_2^+ (formed in situ from Me_2PCl and TMSOTf, see Scheme 2c) gives [(P*t*Bu)$_3$PMe$_2$][OTf] (**4b**-OTf) almost quantitatively through a PMe_2^+ bond insertion/ring expansion process. The complicated ^{31}P NMR spectrum of **4b**-OTf (Figure 1c) was simulated at 101.3 MHz (Figure 1c, inverted) and at 202.6 MHz as a second-order AB_2X spin system and is consistent with the symmetric *meso* structure of **4b** observed in the solid state (Figure 2c). There is no evidence for the existence of the diastereomeric isomers of **4b**, thus indicating a stereospecificity of the reaction that can be rationalized in terms of "PMe_2^+" insertion into the *syn*-configured P–P bond at the less-hindered face of **6a**,[20] as observed in similar insertions of "PCl" and "PBr".[21]

Examples of cations based on framework **4** have been previously postulated on the basis of elemental analysis[22,23] and ^{31}P NMR data;[24] however, we provide herein the first confirmation of structural types **3** and **4**. The solid-state structural features of **3a**-OTf, **4a**-OTf, and **4b**-OTf are listed in Table 1 along with the comparative parameters of [P_5Ph_6][OTf] (**5a**-OTf), **6a**, **7**, and (PPh)$_5$. The methylated, four-coordinate P1 center in **3a** is significantly distorted with the C-P1-P angles exhibiting the widest range (108.6–133.2°) of the compounds listed in Table 1 (Figure 2a). Whereas the endocyclic angles in **3a** are similar to those in the neutral precursor **6a**, the plane defined by C1,P1,C2 is twisted by 72.49(6)° with respect to the plane of the three phosphorus atoms (ideally 90°) because of the steric interactions of the *syn* substituents. The greater steric imposition of the *tert*-butyl substituents in **4b** relative to that of the cyclohexyl substituents in **4a** is indicated by both the greater planarity of the P_4 ring in **4b** (P-P-P-P torsional angles: **4a**: 23.6–24.2°, **4b**: 10.3–10.5°; c.f. (P*t*Bu)$_4$: 24.5°, **7**: 31.4°) and a greater distortion of the tetrahedral geometry at P1 in **4b**, in which a larger range of C-P1-P angles and a smaller C-P-C angle are adopted (Table 1). In this context, the cyclohexyl substituent at P1 in **4a** minimizes steric interactions by twisting to enable a *gauche* conformation of the α-hydrogen atom of C2 and the methyl substituent (C1).

The P–P distances are remarkably regular in neutral, anionic, and cationic compounds, although the four-coordinate phosphorus centers of the cations typically form slightly shorter P–P bonds (bold values in column 3 of Table 1). Interestingly, the P–P distances between the three-coordinate phosphorus centers in the cations are somewhat longer than those in the neutral cyclopolyphosphines. Consistent with the trend in P–P distances, the shortest P–C bonds within a given cation involve the phosphonium center (bold values in column 2 of Table 1).

Table 1: Selected distances [Å] and angles [°] for **3a**-OTf, **4a**-OTf, and **4b**-OTf, and the comparative features of **5a**-OTf, **6a**, **7**, and $(PPh)_5$.[a]

Compound	P–C	P–P	C-P-P	C-P-C	P-P-P	Ref.
$[(PtBu)_3Me][OTf]$	**1.858(2) [1,2]**	**2.1465(6) [1,2]**	**123.15(7) [1,1,2]**	**110.41(9)** [1,1,2]	**62.31(2) [2,1,3]**	[b]
(**3a**-OTf)	**1.806(2) [1,1]**	**2.1652(6) [1,3]**	**108.62(7) [1,1,3]**		59.26(2) [1,2,3]	
	1.886(2) [2,6]	2.2306(6) [2,3]	**112.97(6) [2,1,2]**		58.43(2) [1,3,2]	
	1.894(2) [3,10]		**133.21(6) [2,1,3]**			
$[(PCy)_4Me][OTf]$	**1.822(2) [1,2]**	**2.1952(6) [1,2]**	**114.45(7) [1,1,2]**	**108.44(8) [1,1,2]**	**91.05(2) [4,1,2]**	[b]
(**4a**-OTf)	**1.797(2) [1,1]**	**2.1896(6) [1,4]**	**115.54(7) [1,1,4]**		84.92(2) [1,2,3]	
	1.867(2) [2,8]	2.2387(6) [2,3]	**113.68(6) [2,1,2]**		88.68(2) [4,3,2]	
	1.871(2) [3,14]	2.2378(6) [3,4]	**113.03(6) [2,1,4]**		85.07(2) [1,4,3]	
	1.858(2) [4,20]					
$[(PtBu)_3PMe_2][OTf]$ (**4b**)	**1.800(2) [1,2]**	**2.2032(5) [1,2]**	**106.33(6) [1,1,2]**	**105.99(9) [2,1,1]**	**94.33(2) [4,1,2]**	[b]
	1.802(2) [1,1]	**2.1983(6) [1,4]**	**105.12(6) [1,1,4]**		85.50(2) [1,2,3]	
	1.890(2) [2,3]	2.2385(6) [2,3]	**120.56(6) [2,1,4]**		92.47(2) [4,3,2]	
	1.890(2) [3,7]	2.2307(6) [3,4]	**122.72(6) [2,1,2]**		85.80(2) [1,4,3]	
	1.885(2) [4,11]					
$[P_5Ph_6][OTf]$ (**5a**)	**1.798(2)**	**2.2221(6)**	**106.08(6)**	**111.59(8)**	**107.36(2)** 96.52(2)	[18]
	1.799(2)	**2.2072(6)**	**113.22(6)**		93.59(2)	
	1.829(2)	2.2318(6)	**111.57(6)**		89.56(2)	
	1.843(2) 1.842(2)	2.2392(6)	**107.03(6)**		91.64(2)	
	1.827(2)	2.2251(6)				
$(PtBu)_3$ (**6a**)[c]	1.874(5)	2.188(2) 2.186(2) 2.216(2)	105.0–123.7	–	60.8(1) 59.6(1) 59.6(1)	[20]
	1.915(5)		av. 112.1			
	1.897(5)					
$(PCy)_4$ (**7**)	1.874(2)	2.224(2)	102.8(1)	–	85.47(6)	[25]
			102.6(1)			
$(PPh)_5$	1.83(1)–6(1)	2.207(5)–23(5)	96.4(4)–109.8(4)	–	94.0(2)–107.2(2)	[26]
	av. 1.84	av. 2.217	av. 102.0		av. 100.0	

[a] Numbers in square brackets denote atom labels and the values in bold are those that involve the four-coordinate phosphorus center (av. = average value). [b] This work. [c] The average of two crystallographically independent molecules.

In a preliminary study of reactivity, reaction mixtures that contain **4a**-OTf and PMe_3 show the characteristic A_2B pattern of $(PCy)_3$ (**6c**) in the ^{31}P NMR spectra.[27] In addition, two new doublets ($\delta = 15.4$ and -38.2 ppm, $^1J(P\text{-}P) = 295$ Hz) are assigned to the new phosphinophosphonium cation in $[Me_3P\text{-}PMeCy][OTf]$ (**1a**-OTf), and a low-intensity sharp signal at $\delta = -67$ ppm is assigned to **7** (Scheme 3). The

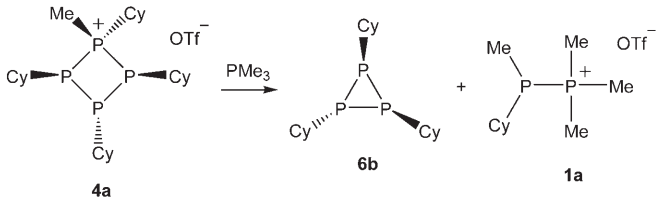

Scheme 3. Phosphenium abstraction from **4a**.

abstraction of $MeCyP^+$ from **4a** by PMe_3 effects a ring contraction and, in conjunction with a previous methylation step, highlights a synthetically viable transformation from cyclotetraphosphine $(PR)_4$ to cyclotriphosphine $(PR)_3$. In addition, the reversibility of the phosphenium P–P insertion is observed (by ^{31}P NMR spectroscopic analysis) in the reaction of **4b** with PMe_3, which slowly gives **6a** and $[Me_3P\text{-}PMe_2][OTf]$ (**1b**-OTf).

In summary, the application of methylation or phosphenium insertion reactions to cyclopolyphosphines has enabled the characterization of a family of small cyclopolyphosphinophosphonium monocations. The high-yielding preparations of cyclodiphosphinophosphonium **3** and cyclotriphosphinophosphonium **4** cations are facilitated by the appropriate imposition of substituent steric strain in the starting cyclopolyphosphines. The phosphenium abstraction induced by PMe_3 and ring contraction provides further systematic development of these fundamentally important *catena*-phosphorus frameworks.

Experimental Section

Small-scale reactions were carried out in a glove box with an inert N_2 atmosphere. Solvents were dried on an MBraun solvent-purification system and stored over molecular sieves prior to use. $(PtBu)_3$[28] and $(PCy)_4$[29] were prepared according to literature methods. All the reported ^{31}P NMR parameters were derived by computer simulation, as all compounds exhibited some degree of second-order character.

3a-OTf: MeOTf (0.08 mL, 0.71 mmol) was added dropwise to a solution of $(PtBu)_3$ (0.096 g, 0.36 mmol) in fluorobenzene (4 mL). The reaction mixture was filtered after 15 min. Slow diffusion of hexane vapors into the filtrate at −25 °C gave colorless crystals; yield = 0.14 g (0.32 mmol, 87 %). M.p. 121–125 °C; elemental analysis (%) calcd for $C_{14}H_{30}F_3O_3P_3S$: C 39.3, H 7.1; found: C 39.5, H 7.0; ^1H NMR (500.1 MHz, $CDCl_3$, 298 K): $\delta = 3.6$ (dd, $J(P,H) = 13$ Hz, $J(P,H) = 8$ Hz, 1H), 1.6 (d, $^3J(P,H) = 22$ Hz, 3H), 1.4 (d, $^3J(P,H) = 17$ Hz, 3H), 1.6 ppm (d, $^3J(P,H) = 17$ Hz, 3H); ^{31}P NMR (101.3 MHz, $CDCl_3$, 298 K): AMX spin system, $\delta A = -110.3$, $M = -50.8$, $X = -20.4$ ppm, $J(A,M) = -123$, $J(A,X) = -334$, $J(M,X) = -317$ Hz; FTIR (nujol, ranked intensities): $\tilde{\nu} = 1399$ (9), 1260 (1), 1151 (2), 1030 (4), 904 (5), 800 (10), 751 (8), 638 (3), 572 (7), 516 (6) cm^{-1}.

4a-OTf: MeOTf (0.095 mL, 0.84 mmol) was added dropwise to a mixture of $(PCy)_4$ (0.25 g, 0.55 mmol) in CH_2Cl_2 (5 mL). The reaction mixture was filtered after 90 min, and removal of the solvent in vacuo gave a white solid that was recrystallized at −25 °C from fluoroben-

zene by vapor diffusion of hexane over 3 days; yield = 0.15 g (0.23 mmol, 43 %). M.p. 175–177 °C; elemental analysis (%) calcd for $C_{26}H_{47}F_3O_3P_4S$: C 50.3, H 7.6; found: C 50.4, H 7.3; ^{1}H NMR (500.1 MHz, $CDCl_3$, 298 K): $\delta = 2.6$ (m, 1H) 2.4 (d, J(P,H) = 12 Hz, 3H), 2.4 (m, 2H), 1.7–2.1 (m, 20H), 1.1–1.5 ppm (m, 21H); ^{31}P NMR (202.6 MHz, $CDCl_3$, 298 K): A_2MX spin system, $\delta A = -69.8$, M = −56.2, X = 10.1 ppm, ^1J(A,M) = −122, ^1J(A,X) = −230, ^2J(M,X) = −17 Hz; FTIR (nujol, ranked intensities): $\tilde{\nu} = 1284$ (4), 1246 (1) , 1158 (5), 1083 (3), 926 (9), 883 (8), 754 (10), 636 (2), 572 (7), 527 (6) cm^{-1}. Crystals suitable for X-ray diffraction were obtained by vapor diffusion of fluorobenzene/hexane at room temperature.

4b-OTf: A solution of PMe_2Cl (0.044 mL, 0.55 mmol) and TMSOTf (0.10 mL, 0.67 mmol) in CH_2Cl_2 (3 mL) was added dropwise to a solution of (P*t*Bu)$_3$ (0.098 g, 0.37 mmol) in CH_2Cl_2 (3 mL). The solvent was removed in vacuo after stirring of the reaction mixture for 45 min, and the resulting white solid was washed with portions of hexane (2 × 4 mL). The product was recrystallized from fluorobenzene by diffusion of hexane vapor into the solution at room temperature over 5 days; yield = 0.095 g (0.20 mmol, 54 %). M.p. 112–114 °C; elemental analysis (%) calcd for $C_{15}H_{33}F_3O_3P_4S$: C 38.0, H 7.0; found: C 38.5, H 6.9; ^{1}H NMR (500.1 MHz, $CDCl_3$, 298 K): $\delta = 2.7$ (d, ^2J(P,H) = 14 Hz, 1H), 2.4 (dt, J(P,H) = 13 Hz, J(P,H) = 8 Hz, 1H), 1.5 (m, 6H), 2.7 ppm (d, ^3J(P,H) = 14 Hz, 3H); ^{31}P NMR (101.3 MHz, $CDCl_3$, 298 K): AB_2X spin system, $\delta A = -28.2$, B = −24.2, X = −2.1 ppm, ^1J(A,B) = −143, ^1J(B,X) = −251, ^2J(A,X) = 28 Hz; FTIR (nujol, ranked intensities): $\tilde{\nu} = 1304$ (6), 1267 (2), 1224 (7), 1155 (3), 1032 (4), 957 (8), 914 (9), 638 (1), 573 (10), 517 (5) cm^{-1}.

X-ray crystallographic analysis: Data was collected on Bruker AXS P4/SMART 1000 diffractometer using ω and θ scans with a width of 0.3°, a exposure time of 10 s at 173 K, and a detector distance of 5 cm. The data were reduced (SAINT)[30] and corrected for absorption (SADABS).[31] Structures were solved by direct methods and refined by full-matrix least squares on F^2 (SHELXL).[32] All non-hydrogen atoms were refined anisotropically. **3a**-OTf: $C_{14}H_{30}F_3O_3P_3S$; colorless, plates, crystal size 0.40 × 0.40 × 0.10 mm^3, monoclinic, space group $P2_1/n$, $a = 13.6318(9)$, $b = 10.5918(7)$, $c = 15.487(1)$ Å, $\beta = 104.084(1)°$, $V = 2168.9(2)$ Å^3, $Z = 4$, $\mu = 0.405$ mm^{-1}; $\lambda(Mo_{K\alpha}) = 0.71073$ Å, $2\theta_{max.} = 53.8°$, collected (independent) reflections = 14573 (4869), $R_{int} = 0.0213$; 337 refined parameters, $R_1 = 0.0487$, $wR_2 = 0.1056$ for all data, max./min. residual electron density = 0.646/−0.476 e Å^{-3}. **4a**-OTf: $C_{26}H_{47}F_3O_3P_4S$, colorless parallelepiped, crystal size 0.275 × 0.20 × 0.175 mm^3, triclinic, space group $P\bar{1}$, $a = 11.4946(7)$, $b = 11.5640(7)$, $c = 14.0822(9)$ Å^3, $\alpha = 110.984(1)$, $\beta = 102.476(1)$, $\gamma = 106.868(1)°$, $V = 1561.62(17)$ Å^3, $Z = 2$, $\mu = 0.352$ mm^{-1}; $\lambda(Mo_{K\alpha}) = 0.71073$ Å, $2\theta_{max.} = 52.2°$, collected (independent) reflections = 10965 (6795), $R_{int} = 0.0195$; 522 refined parameters, $R_1 = 0.0475$, $wR_2 = 0.0964$ for all data, max./min. residual electron density = 0.491/−0.247 e Å^{-3}. **4b**-OTf: $C_{15}H_{33}F_3O_3P_4S$, colorless parallelepiped, crystal size 0.40 × 0.275 × 0.25 mm^3, tetragonal, space group $I4_1/a$, $a = 25.6452(11)$, $b = 25.6452(11)$, $c = 14.7549(8)$ Å^3, $V = 9703.9(8)$ Å^3, $Z = 16$, $\mu = 0.432$ mm^{-1}; $\lambda(Mo_{K\alpha}) = 0.71073$ Å, $2\theta_{max.} = 54.7°$, collected (independent) reflections = 33323 (5547), $R_{int} = 0.0293$; 367 refined parameters, $R_1 = 0.0445$, $wR_2 = 0.0809$ for all data, max./min. residual electron density = 0.414/−0.237 e Å^{-3}.

CCDC-271727–271729 (**3a**, **4a**, and **4b**, respectively) contain the supplementary crystallographic data for this paper. These data can be obtained free of charge from the Cambridge Crystallographic Data Centre via www.ccdc.cam.ac.uk/data_request/cif.

Received: May 27, 2005
Published online: August 31, 2005

[1] K. B. Dillon, F. Mathey, J. F. Nixon, *Phosphorus: The Carbon Copy*, Wiley, New York, **1997**.
[2] M. Baudler, *Angew. Chem.* **1982**, *94*, 520; *Angew. Chem. Int. Ed. Engl.* **1982**, *21*, 492–512.
[3] M. Baudler, *Angew. Chem.* **1987**, *99*, 429; *Angew. Chem. Int. Ed. Engl.* **1987**, *26*, 419–441.
[4] M. Baudler, K. Glinka, *Chem. Rev.* **1993**, *93*, 1623–1667.
[5] M. Baudler, K. Glinka, *Chem. Rev.* **1994**, *94*, 1273–1297.
[6] A. Schisler, P. Lonnecke, T. Gelbrich, E. Hey-Hawkins, *Dalton Trans.* **2004**, 2895–2898.
[7] A. Schisler, P. Lonnecke, U. Huniar, R. Ahlrichs, E. Hey-Hawkins, *Angew. Chem.* **2001**, *113*, 4345–4348; *Angew. Chem. Int. Ed.* **2001**, *40*, 4217–4219.
[8] R. Wolf, E. Hey-Hawkins, *Chem. Commun.* **2004**, 2626–2627.
[9] R. Wolf, A. Schisler, P. Lonnecke, C. Jones, E. Hey-Hawkins, *Eur. J. Inorg. Chem.* **2004**, 3277–3286.
[10] H.-W. Lerner, G. Margraf, L. Kaufmann, J. W. Bats, M. Bolte, M. Wagner, *Eur. J. Inorg. Chem.* **2005**, 1932–1939.
[11] H.-W. Lerner, M. Bolte, K. Karaghiosoff, M. Wagner, *Organometallics* **2004**, *23*, 6073–6076.
[12] N. Wiberg, A. Wörner, H.-W. Lerner, K. Karaghiosoff, D. Fenske, G. Baum, A. Dransfeld, P. v. R. Schleyer, *Eur. J. Inorg. Chem.* **1998**, 833–841.
[13] A. Schmidpeter, S. Lochschmidt, W. S. Sheldrick, *Angew. Chem.* **1985**, *97*, 214; *Angew. Chem. Int. Ed. Engl.* **1985**, *24*, 226–227.
[14] A. Schmidpeter, S. Lochschmidt, K. Karaghiosoff, W. S. Sheldrick, *J. Chem. Soc. Chem. Commun.* **1985**, 1447–1448.
[15] A. Schmidpeter, S. Lochschmidt, *Angew. Chem.* **1986**, *98*, 271; *Angew. Chem. Int. Ed. Engl.* **1986**, *25*, 253–254.
[16] L. Heuer, L. Ernst, R. Schmutzler, D. Schomburg, *Angew. Chem.* **1989**, *101*, 1549; *Angew. Chem. Int. Ed. Engl.* **1989**, *28*, 1507–1509.
[17] N. Burford, P. J. Ragogna, R. McDonald, M. Ferguson, *J. Am. Chem. Soc.* **2003**, *125*, 14404–14410.
[18] N. Burford, C. A. Dyker, A. Decken, *Angew. Chem.* **2005**, *117*, 2416–2419; *Angew. Chem. Int. Ed.* **2005**, *44*, 2364–2367.
[19] Spin systems are labeled from the lowest frequency excitation (designated A) to the highest (designated X).
[20] J. Hahn, M. Baudler, C. Kruger, Y.-H. Tsay, *Z. Naturforsch. B* **1982**, *37*, 797–805.
[21] B. Riegel, A. Pfitzner, G. Heckmann, H. Binder, E. Fluck, *Z. Anorg. Allg. Chem.* **1995**, *621*, 1365–1372.
[22] R. Appel, R. Milker, *Z. Anorg. Allg. Chem.* **1975**, *417*, 161–170.
[23] K. Issleib, C. Rockstroh, I. Duchek, E. Fluck, *Z. Anorg. Allg. Chem.* **1968**, *360*, 77–87.
[24] K. K. Laali, B. Geissler, M. Regitz, *J. Org. Chem.* **1995**, *60*, 3149–3154.
[25] J. C. J. Bart, *Acta Crystallogr. Sect. B* **1969**, *25*, 762.
[26] J. J. Daly, *J. Chem. Soc. Suppl.* **1964**, 6147–6166.
[27] M. Baudler, C. Pinner, C. Gruner, J. Hellmann, M. Schwamborn, B. Kloth, *Z. Naturforsch. B* **1977**, *32*, 1244–1251.
[28] M. Baudler, K. Glinka, *Inorg. Synth.* **1989**, *25*, 1–5.
[29] W. A. Henderson, M. Epstein, F. S. Seichter, *J. Am. Chem. Soc.* **1963**, *85*, 2462–2466.
[30] SAINT 6.02, Bruker AXS, Inc., Madison, Wisconsin, USA, **1997–1999**.
[31] SADABS George Sheldrick, Bruker AXS, Inc., Madison, Wisconsin, USA, **1999**.
[32] SHELXTL 6.14, Bruker AXS, Inc., Madison, Wisconsin, USA, **2000–2003**.

Keywords: catenation · cations · phosphines · phosphorus · polycations

